COBEM 2023 27TH INTERNATIONAL CONGRESS OF MECHANICAL ENGENEERING

ABCM Brazilian Society of Mechanical Sciences and Engineering
27th ABCM International Congress of Mechanical Engineering
December 04-08, 2023, Florianópolis-SC, Brazil

COB-2023-1669
COLLAPSE OF SUBSEA PIPELINES: NUMERICAL STUDY ON THE INTERACTION OF CORROSION DEFECTS WITH DIFFERENT GEOMETRIC PROPERTIES

Savanna Cristina Medeiros D'Aguiar
Silvana Maria Bastos Afonso da Silva
Civil Engineering Department, Federal University of Pernambuco (UFPE), Av. Acadêmico Hélio Ramos, S/N, 50740-550 Recife, Brazil.
savanna.cristina@ufpe.br
silvana.bastos@ufpe.br

Renato de Siqueira Motta
Civil Engineering Department, Federal University of Pernambuco (UFPE), Av. Acadêmico Hélio Ramos, S/N, 50740-550 Recife, Brazil.
renato.motta@ufpe.br

Abstract. *Subsea pipeline integrity and risk management is a constant challenge due to the hostile environment and operational conditions changes. These pipelines are usually subjected to corrosion attacks. The corrosion geometry is random and can be modeled as a single defect or a group of defects. Multiple corrosion defects can interact with each other and significantly affect the resistance capacity of corroded pipelines. The spacing between defects plays an important role, as when it increases, the interaction between defects decreases. However, the interaction rules also depend on the mutual orientation of the defects, their geometry, and other parameters. The Finite Element (FE) Method has been widely used to evaluate the residual strength of corroded pipelines. Numerical FE analyses present efficient and reliable results and allow extensive parametric studies. This paper evaluates the influence of the spacing between corrosion defects with different sizes on the resistance to the collapse of subsea pipelines under high external pressure. Nonlinear analyses will be performed using the PIPEFLAW system, developed by the PADMEC (High-Performance Processing in Computational Mechanics) research group from UFPE (Federal University of Pernambuco). The PIPEFLAW integrates various tools for automatic FE model generation and FE analysis. The generated FE models were validated against experimental results available in the literature, and a good agreement was reached. After validation, sensitivity studies are conducted on interaction mechanisms for various parameters, considering dual defects with different geometrical properties positioned longitudinally. In general, it is found that the size of the defect has the most significant influence on the interaction between defects. Other factors, such as pipe characteristics and initial ovality, are essential in defect interaction rules. Thus, the results obtained in this study can contribute to advancing knowledge about the effects of interactive defects of different sizes on the collapse resistance of subsea pipelines.*
Keywords: *Collapse pressure, External pressure, Corrosion, Defect interaction rules, Numerical simulation.*

1. INTRODUCTION

Subsea pipelines play an essential role in efficiently and safely transporting oil and gas. Corrosion stands out among the main degradation mechanisms of these elements (Amaya-Gómez et al., 2019). Corrosion is responsible for 36% of pipeline failures (Liu et al., 2018) and can cause accidents of great magnitude with economic, environmental, and humanitarian repercussions. In ultra-deepwater scenarios, reducing the pipe wall thickness due to corrosion can cause collapse under external pressure rather than bursting under internal pressure (Drumond et al., 2018).

The behavior of subsea pipelines with single corrosion defects subjected to external pressure has consolidated research (Benjamin and Cunha 2015; Fan et al. 2017; Fraldi et al. 2011; Fraldi and Guarracino 2011; Gong et al. 2021; Kara, Navarro, and Allwood 2010; Netto 2009; Netto, Ferraz, and Botto 2007; Papadakis 2008; Sakakibara, Kyriakides, and Corona 2008; Xue and Gan 2014; Yan, Shen, and Jin 2015; Ye, Yan, and Jin 2016). However, in real pipelines, corrosion defects are usually present in clusters, and the interaction between these defects can significantly affect the pipeline's failure mode and collapse capability (Li et al., 2016). Therefore, studies on the collapse response of pipelines with multiple corrosion defects have received significant attention.

Interactive defects occur when the spacing between them is small enough to allow interaction in the longitudinal, circumferential, or both directions. Interaction rules can determine a critical spacing between corrosion defects, from which, for simulation purposes, defects can be considered isolated, i.e., the interaction effect can be ignored if the spacing between defects exceeds this critical value (Qin and Cheng, 2021).

DNV (2017) is useful for evaluating interacting defects. However, the interaction rules specified are strictly valid for defects subject only to internal pressure. In the literature, research on interacting defects focuses mainly on pipelines subjected to internal pressure, and several papers can be found on this topic (Al-Owaisi et al., 2016; Benjamin et al., 2005, 2016; Chouchaoui and Pick, 1996; Idris et al., 2021; Li et al., 2016; Mondal and Dhar, 2017; Motta et al., 2017; Silva et al., 2007).

On the other hand, studies on the interaction mechanisms for pipelines subjected to external pressure are still scarce, and there are gaps in establishing interaction rules to be used in these cases. Gong et al. (2020b) evaluated collapse evolution considering pipelines with two identical defects on the external surface. Experimental tests were conducted and will be used as a basis for the present study. Moreover, in Gong et al. (2020b), finite element models were developed, and extensive parametric analyses were conducted. The authors found that the geometric characteristics of the pipeline and the defect parameters play an important role in the interaction rules. At the same time, the primary material properties have a relatively small influence.

Wu et al. (2022) also conducted an extensive parametric study to determine the main factors affecting the interaction of corrosion defects in subsea pipelines. They proposed a formula for the collapse pressure of the pipeline with interacting corrosion defects. The results obtained in this investigation revealed that the defects location is a vital parameter affecting the collapse response.

This paper investigates the interaction between two corrosion defects of subsea pipelines under external pressure, considering different geometric properties of the pipeline and the defects. The nonlinear FE analyses are performed using the models generated by the PIPEFLAW automatic modeling tool, developed by the PADMEC (High-Performance Processing in Computational Mechanics) research group at the Federal University of Pernambuco (UFPE, Brazil). PIPEFLAW is a computational tool based on MSC.PATRAN (PATRAN, 2012) software integrates several tools for automatic FE model generation and FE analysis via ANSYS (2020). Several studies have been developed considering this tool and have presented accurate and reliable results for evaluating the integrity of corroded pipelines (Bruère et al., 2019; Cabral et al., 2007, 2017; Ferreira et al., 2021; Motta et al., 2017, 2021; Pimentel et al., 2020; Soares et al., 2019).

2. FINITE ELEMENT MODELING

The meshes used in this paper are generated using 3D hexahedral solid elements created from the PIPEFLAW system. The discretization used is available on the standard procedure described in detail by Cabral et al. (2007, 2017). Overall, a refined mesh was used in the defect region, and less refined intermediate meshes were used in the regions further away from the defect, including transition regions along the thickness, transition regions along the surface, and mesh expansion regions. The distribution and refinement of the elements varied depending on the defect geometry.

2.1 Material Properties

The material to be considered in the numerical examples is the material of the specimens used in the uniaxial tensile tests described by Gong et al. (2020b). Figure 1 shows the material stress-strain curve constructed from the modified Ramberg-Osgood model (Gong et al., 2020a). The modified Ramberg-Osgood (R-O) model which can be expressed as:

$$\varepsilon = \frac{\sigma}{E}\left(1 + \frac{3}{7}\left|\frac{\sigma}{\sigma_y}\right|^{n-1}\right), \tag{1}$$

where ε, σ, E, σ_y and n are the uniaxial strain, the uniaxial stress, the elastic modulus, the effective yield stress, and the strain hardening parameter, respectively.

According to Gong et al. (2020a), Equation 1 is used only for strain values less than 0.015. For strain levels greater than 0.015, the stress-strain response exhibits a linear relationship, whose slope is given by:

$$E' = \left.\frac{d\sigma}{d\varepsilon}\right|_{\varepsilon=0.015} = E\left(1 + \frac{3}{7}n\left|\frac{\sigma}{\sigma_y}\right|^{n-1}\right)^{-1}, \tag{2}$$

where E' is the material's modulus of hardening.

The basic mechanical properties of the material were listed as follows: E = 200 GPa, σ_y = 198.2 MPa, n = 8.9, E' = 2400 MPa, $\sigma_{0.5}$ = 252.8 MPa (yield stress at a strain of 0.5%). The von Mises equivalent stress is used to represent the state of multi-axial stress in a single positive stress.

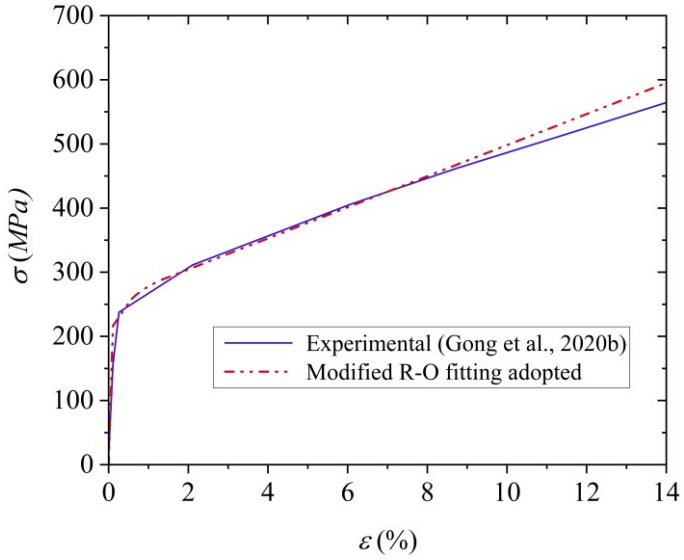

Figure 1. Stress-strain curve of pipe material.

2.2 Load and boundary conditions

Figure 2 illustrates all the boundary and load conditions generated by the PIPEFLAW system for the cases where symmetry is not considered. Boundary conditions are applied to restrict the displacements in the longitudinal direction (Fix *Z*) at the ends of pipes. The displacement at θ (angular cylindrical coordinate) direction is also restricted (Fix θ) to avoid rigid body motion (rotation).

The PIPEFLAW system allows the application of several loads (internal pressure, external pressure, axial force, bending moment). However, as already mentioned, the models generated in this study are subjected only to external pressure. In future studies, it is intended to expand the collapse analysis considering the combination of other loads.

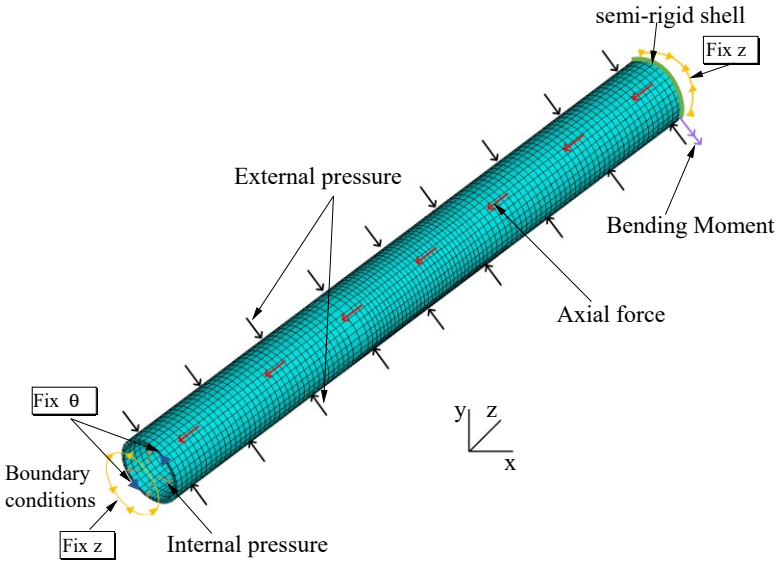

Figure 2. Loads and boundary conditions in the pipeline allowed by PIPEFLAW.

3. NON-LINEAR ANALYSIS

Nonlinear analyses in the present work were performed using the commercial software ANSYS (2020). The collapse response of a thick-walled steel pipe involves severe geometric nonlinearities and structural instability (Gong et al., 2020b).

In collapse simulations, the hydrostatic collapse pressure is the maximum pressure the pipeline reaches in a geometric non-linear elastoplastic analysis. The Riks method (Riks, 1972) with automatic arc length adjustment was adopted here to follow the proportional load history. In each analysis step, the external pressure is incremented using a load factor, and the NLGEOM, specification available in ANSYS (2020), was set to "ON" to account for geometric nonlinearity.

4. VALIDATION

The collapse responses of the pipes are analyzed and validated based on the experimental results of Gong et al. (2020b). These authors considered three types of elliptical defect arrangements on the outer surface of the pipes: (1) two longitudinally positioned defects, (2) two circumferentially positioned defects, and (3) two diagonally positioned defects. The schematic diagram of the three defect arrangements is shown in Figure 3.

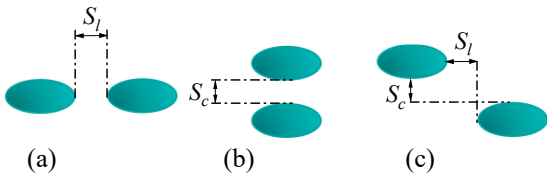

Figure 3. Corrosion defects at different arrangements (a) Longitudinally (b) Circumferentially (c) Diagonally.

In all cases, the outer diameter (D) and the wall thickness (t) of the pipeline are 83 and 4 mm, respectively. In the present study, the pipeline length is modeled as ten times the outer diameter of the pipe to avoid the influence of boundary conditions on the results of the analyses. The length l, circumferential width c, and depth d were 83 mm, 13.04 mm, and 2.4 mm, respectively, for all corrosion defects, according to Gong et al. (2020b).

Elliptical and rectangular models are developed to simulate the experiments of Gong et al. (2020b). In elliptical models, the actual geometric parameters of the experiment are used (Exact Model). On the other hand, in the rectangular models, the defect regions are idealized with constant length, width, and thickness (Simplified Model). Figure 4 presents the rectangular model adopted in this study for the three types of defect arrangements.

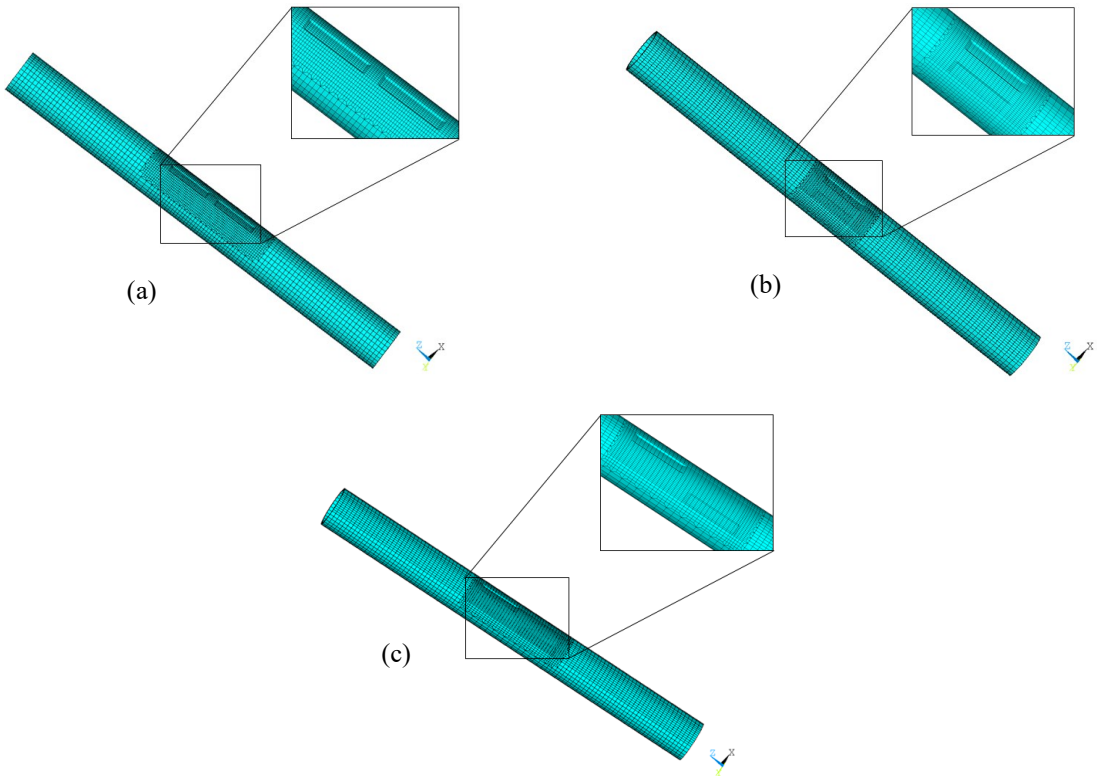

Figure 4. Schematic diagram of finite element mesh at different defects arrangements:(a) Longitudinally (b) Circumferentially (c) Diagonally.

In both defect geometries, the defect orientation and the initial ovality (Δo = 0.1%) agree with the experiments of Gong et al. (2020b). The initial ovality was inserted after the model generation using coordinate transformation. More details on the consideration of the ovalization procedure in the PIPEFLAW are available in Motta et al. (2021).

Table 1 shows the results of calculated collapse pressures and the longitudinal and circumferential spacings between defects for all cases. The results obtained by the FE simulations, elliptical geometry, showed excellent agreement with the experimental results. The most significant discrepancies are observed in the cases of diagonally aligned defects. However, the results obtained from the FE models in the present work for these cases favor safety (conservative).

As expected, the results obtained by the FE model, rectangular geometry, are more conservative than the ones obtained by experimental tests and from the elliptical FE model. According to Netto, Ferraz, and Botto (2007), the degree of conservatism of the rectangular model varies according to the geometry of the defect. The authors justify that as more material is removed from the pipe in the rectangular analysis, the defect, depending on its geometry, tends to have an arch-like behavior. This behavior was previously described by Xue and Fat (2002).

Figure 5 shows the von Misses stress distribution from the elliptical and rectangular models for the TSA2 case. The results obtained from both models capture the correct failure region, and the von Mises stress contours showed good agreement for both cases.

Table 1. Summary of the geometric characteristics of defects and collapse pressures.

Specimen	Aligned type	S_l (mm)	S_c (mm)	$P_{colapsse}$ (MPa)			
				$Exp^{ref\ (1)}$	$FE^{ref\ (2)}$	$FE^{elliptical\ (3)}$	$FE^{rectangular\ (3)}$
TSA1	Longitudinal	0.00	-	16.12	16.50	16.59	13.02
TSA2	Longitudinal	20.00	-	16.78	16.80	17.02	14.24
TSA3	Longitudinal	55.00	-	17.45	17.12	17.29	14.44
TSA4	Longitudinal	80.00	-	17.70	17.24	17.39	14.49
TSC1	Circumferential	-	0.00	16.52	16.48	16.62	11.86
TSC2	Circumferential	-	20.00	18.78	18.05	18.25	14.95
TSC3	Circumferential	-	55.00	17.39	17.47	17.46	14.83
TSC4	Circumferential	-	80.00	16.90	16.94	17.20	14.55
TSD1	Diagonal	0.00	0.00	17.01	17.54	16.88	13.18
TSD2	Diagonal	20.00	20.00	19.34	18.77	17.56	14.47
TSD3	Diagonal	80.00	80.00	18.87	18.32	17.45	14.76

(1) Collapse pressure from the experimental result by Gong et al (2020b); (2) Collapse pressure predicted by FE simulations conducted by Gong et al (2020b); (3) Collapse pressure from the current FE using PIPEFLAW/ANSYS.

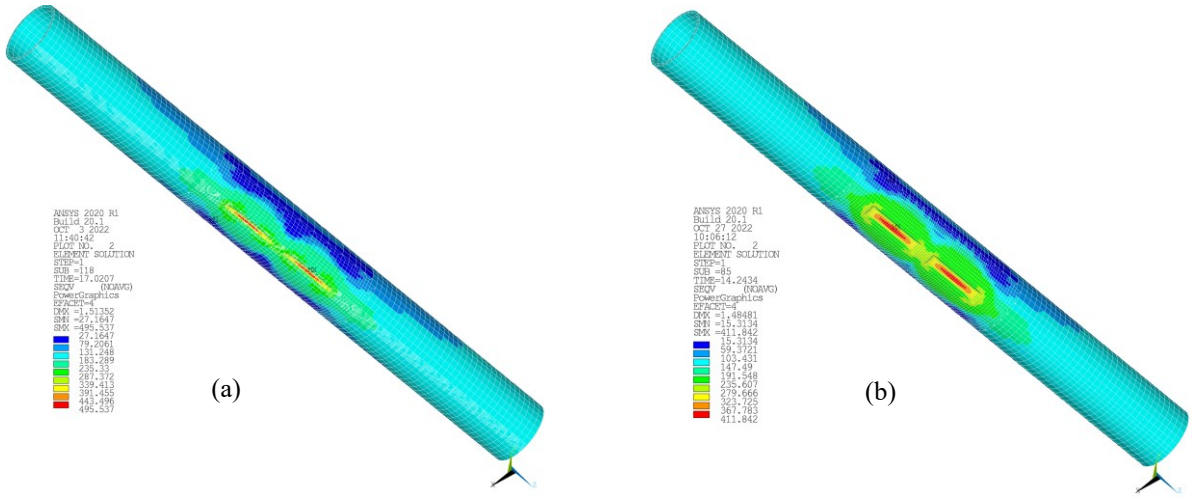

Figure 5. Von Misses stress distribution for specimen TSA2 (a) Elliptical defects (b) Rectangular defects.

5. PARAMETRIC STUDY

This section evaluates the interaction between two corrosion defects, aligned longitudinally, considering different geometric properties of the pipe and the defects. The geometric and material properties are the same as those adopted in the parametric study by Gong et al. (2020b). The geometric parameters are D = 323.85 mm, D/t = 20.4, Δo = 0.1 %, l/D

= 1.0, $c/\pi D$ = 0.005 e d/t = 0.6. The spacings between the defects, normalized for the pipe thickness, are S_l/t = 0, 10, 20, 30, 40, 50. The material to be considered in examples is X65 steel, with E = 207 GPa, σ_y = 410 MPa, n = 13, E' = 3047 MPa, $\sigma_{0.5}$ = 450 MPa. However, in the present work, the influence of these properties in cases where the corrosion defects do not have identical geometries is examined (Figure 6).

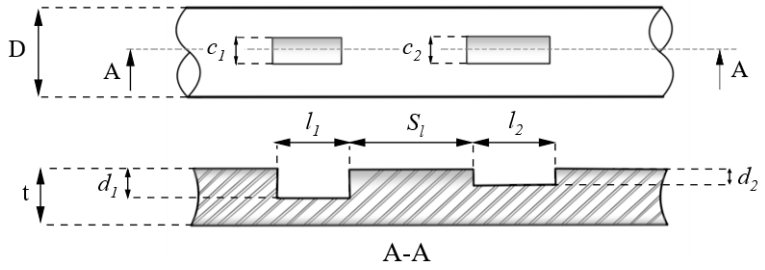

Figure 6. Schematic diagram of dual defects.

The parametric study used the rectangular model to obtain a more conservative approximation of the defects. In the results presented below, the interaction evaluation parameter J (Wu et al. 2022) was used as the ratio $P_{multiple}$ / P_{single} (normalized collapse pressure). $P_{multiple}$ is the collapse pressure of multiple defects, and P_{single} is the collapse pressure of a single defect. Since the defects are not identical in the cases evaluated, P_{single} was considered equal to the collapse pressure of the most critical defect. The presence of interaction between the defects is considered when $P_{multiple}$ is smaller than P_{single}. The criterion used to evaluate the interaction between the defects is described as follows (Gong et al. 2020b; Idris et al. 2021; Wu et al. 2022):

$J \geq 0.99$, *no interaction* (3)

$J < 0.99$, *interaction exists* (4)

When the normalized collapse pressure (interaction evaluation parameter J) reaches a value of 0.99, the spacing between the defects is defined as the critical spacing.

5.1 Effect of defect size on the defects interaction

To evaluate the influence of different defect sizes, the length of defect 2 (l_2) is varied and the collapse response is evaluated by considering the increase in the longitudinal distances between defects. The defect length 1 (l_1) and the other parameters are kept constant. Figure 6 shows the results of varying the defect length considering different depths. For all cases, increasing l_2 results in an increase in the J parameter, indicating that the greater the difference between the defects length, the lower the interaction between them. Furthermore, there is a reduction in the critical spacing when the difference between the defects length increases. Comparing Figures 7 (a) and 7(b), the influence of increasing the defect depth is observed. The critical spacing between defects tends to decrease with increasing defect depth. When d/t increases to 0.6 (Figure 7b), the defect length has less importance on the interaction, especially when considering l_2 greater than l_1.

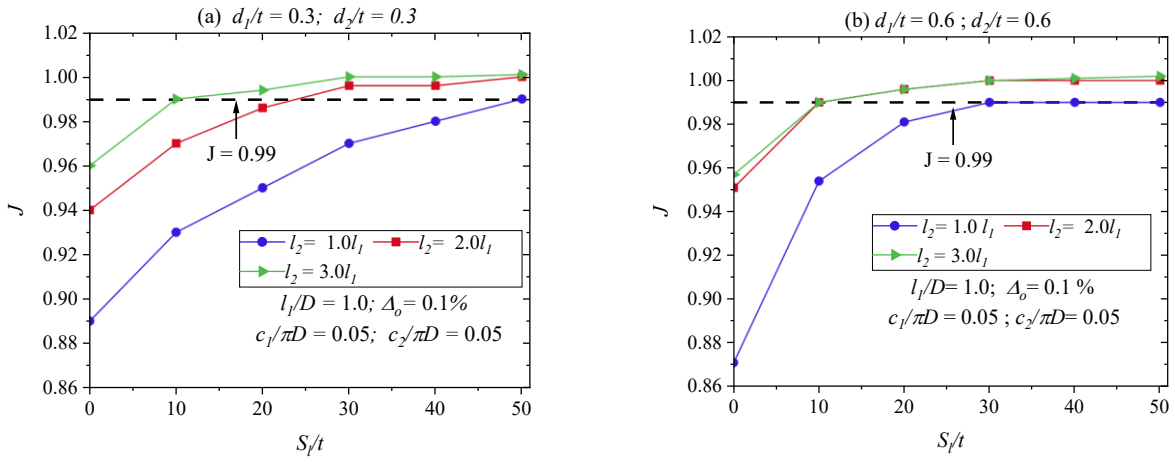

Figure 7. Defect spacing behavior of corroded pipes with different defect lengths: (a) d/t =0.3 and (b) d/t =0.6.

The influence of defect width considering different depths is graphically illustrated in Figure 8. The study considers the increase in the width of defect 2 (c_2) keeping all other parameters constant. Increasing the difference between the defects width leads to an increase in J and consequently reduces the critical spacing value. Regarding defect depth, the pipe with a higher defect depth (Figure 8b) presents a smaller critical spacing for all cases.

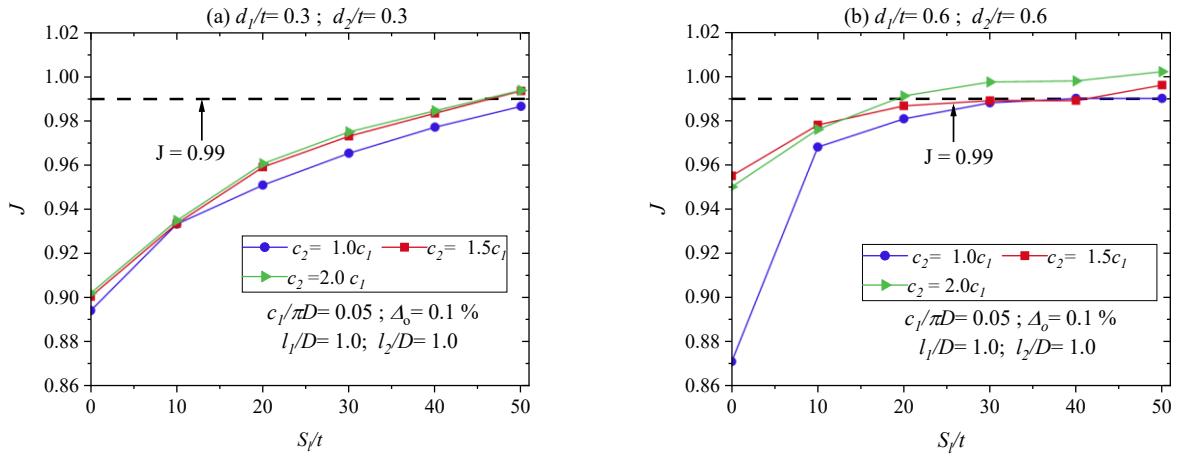

Figure 8. Defect spacing behavior of corroded pipes with different defect widths: (a) d/t =0.3 and (b) d/t =0.6.

The previous results reveal that the defect depth parameter is essential in the collapse response. To evaluate the influence of different defect depths, the depth of defect 2 (d_2) is varied while keeping the depth of defect 1 (d_1) and the other parameters constant. Figure 9 (a) shows that when d_1 is small (d_1/t =0.1), the influence of the increase in d_2 on the interaction rule is insignificant and can be ignored.

For higher defect depth (d_1/t =0.3), shown in Figure 9 (b), the influence of the increase in d_2 has a greater impact on interaction. Note that J increases significantly as defect 2 deepens, reducing the critical spacing. The above observations are closely related to the developed collapse modes since the collapse mode of the pipeline changes according to the depth of the defect, affecting the collapse pressure of the corroded pipes.

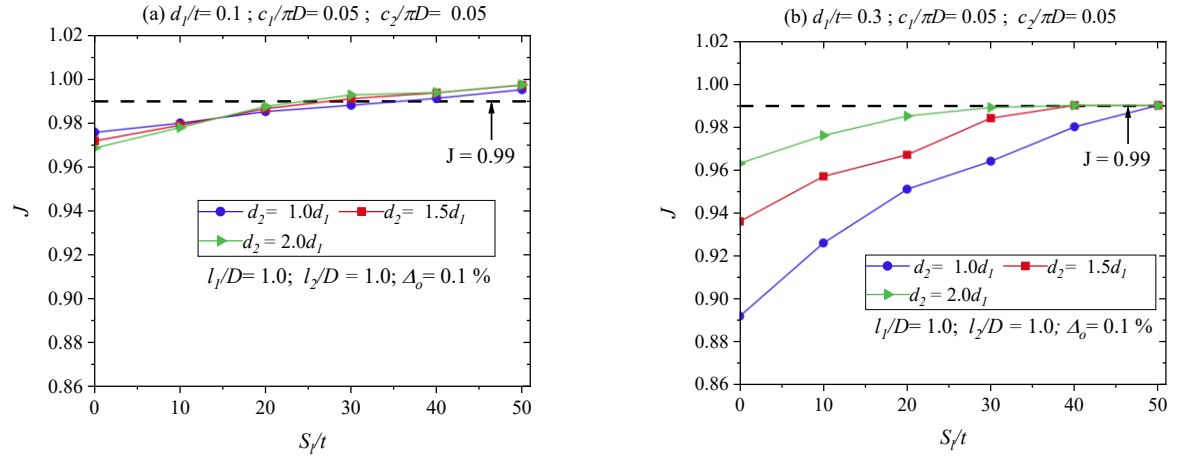

Figure 9. Defect spacing behavior of corroded pipes with different defect depths: (a) d_1/t =0.1 and (b) d_1/t =0.3.

5.2 Effect of diameter-to-thickness ratio on the defects interaction

Different diameter-thickness ratios (D/t) are considered to evaluate their effect on the collapse of corroded pipelines with two defects. The pipe diameter was kept constant in these analyses, and only its thickness was changed. The study involved three D/t ratios, namely, 20.4, 25.5, and 29.1. The defects for all cases are not identical. Figure 10 shows the effect of varying the diameter-thickness ratio for two divergent cases concerning defect depth, $d_2 = 1.5d_1$ (Figure 10a) and $d_2 = 2.0d_1$ (Figure 10b). In both cases, $l_2 = 2.0l_1$ (length of defect 2), and the defect widths of the two defects are the same ($c_2 = c_1$).

Increasing the D/t ratio leads to a decrease in the normalized collapse pressure (J), indicating that the higher the D/t ratio, the more significant the impact of the defect spacing on the collapse response. Thus, a larger D/t ratio corresponds to a larger critical spacing. The increase in the defect depth (Figure 10b) leads to an increase in the J, reducing the critical

spacing for all cases. The effect of the *D/t* ratio on the critical spacing becomes greater with increasing defect depth. Overall, the influence of the *D/t* ratio plays a vital role in the interaction between defects and should not be ignored.

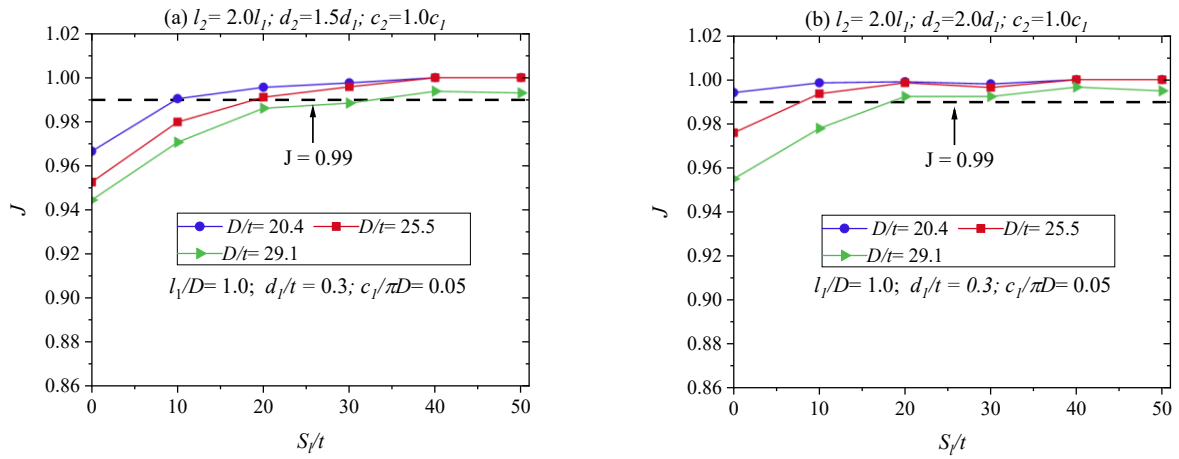

Figure 10. Defect spacing responses of corroded pipes with a different diameter-to-thickness ratio: (a) $d_2 = 1.5d_1$ and (b) $d_2 = 2.0d_1$.

5.3 Effect of initial ovality on the defects interaction

Figure 11 shows the effect of the initial ovality of the pipelines on the defect interaction. Three initial ovalities are adopted in these analyses: 0.1 %, 1.0 %, and 3.0 %. As in the previous analyses, the two corrosion defects are not identical. Figure 11 shows the effect of varying the initial ovality ratio for two divergent cases concerning defect depth, $d_2 = 1.5d_1$ (Figure 11a) and $d_2 = 2.0\ d_1$ (Figure 11b).

The increase in the initial ovality decreases *J* for both cases, indicating an increased interaction between the defects. The deepening of the defect (Figure 11b) causes a reduction in the interaction between the defects. For greater depths, the initial ovality has a more significant impact on the normalized collapse pressure *(J)* and, consequently, on the critical spacing between defects.

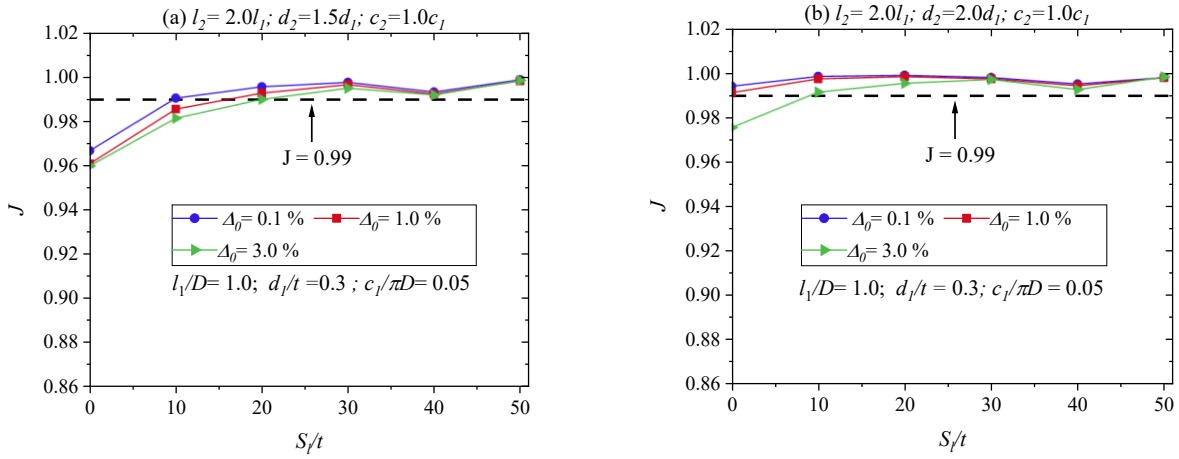

Figure 11. Defect spacing responses of corroded pipes with different initial ovality: (a) $d_2 = 1.5d_1$ and (b) $d_2 = 2.0d_1$.

6. CONCLUSIONS

In this study, finite element models generated by the PIPEFLAW system were initially validated against experimental and numerical results available in the literature, showing excellent agreement. Then, the behavior of two corrosion defects, aligned longitudinally, is analyzed in detail from extensive parametric analyses. Different geometrical properties of the pipeline and the defects were considered. The main conclusions of this study were:

- The parametric study shows, as expected, that increasing the longitudinal spacing between defects leads to decreased interaction.
- The geometric parameters of the corrosion defects play an important role in the interaction rules, especially its depths.

- Other factors, such as the diameter-thickness ratio and initial ovality, had some influence on the interaction rules. This influence becomes more evident for pipelines with deeper corrosion defects.

Finally, the importance of studies about the interaction between corrosion defects in subsea pipelines was highlighted. The results obtained show that different combinations of defect size, pipeline geometric properties, and initial ovality can significantly influence the interaction between defects and, consequently, the pipeline's ability to resist collapse.

7. ACKNOWLEDGEMENTS

The authors would like to thank Petrobras for financially supporting research projects in the pipeline field. The financial support for this research, provided by FACEPE, Grant Program IBPG-1303-3.01/20, is acknowledged, as well as CAPES and CNPq for the financial support of various research projects developed in this area by the PADMEC Research Group.

8. REFERENCES

Al-Owaisi, S. S., Becker, A. A., and Sun, W. 2016. "Analysis of shape and location effects of closely spaced metal loss defects in pressurized pipes", *Engineering Failure Analysis*, vol. 68, p. 172–86.

ANSYS, 2020. Ansys Release 12.0 Documentation: operations guide (Chapter 3) and structural guide (Chapter 8).

Amaya-Gómez, R., Sánchez-Silva, M., and Muñoz, F. 2019. "Integrity assessment of corroded pipelines using dynamic segmentation and clustering", *Process Safety and Environmental Protection*, vol. 128, p. 284–94.

DNV. 2017. Recommended Practice DNV RP-F101 Corroded Pipelines, Det Norske Veritas, Norway.

Benjamin, A. and Cunha, D. 2015. New Method for the Prediction of the Hydrostatic Collapse Pressure of Submarine Pipelines, in *Proceedings of the XXXVI Iberian Latin American Congress on Computational Methods in Engineering*. Rio de Janeiro, Brasil.

Benjamin, A. C., Freire, J. L. F., Vieira, R. D., and Cunha, D. J. S. 2016. "Interaction of corrosion defects in pipelines – Part 2: MTI JIP database of corroded pipe tests", *International Journal of Pressure Vessels and Piping*, vol. 145, p. 41–59.

Benjamin, A. C., Luiz, J., Freire, F., Vieira, R. D., and Diniz, J. L. C. 2005. In *24th International Conference on Offshore Mechanics and Arctic Engineering (OMAE 2005)*. Halkidiki, Greece.

Bruère, V. M., Bouchonneau, N., Motta, R. S., Afonso, S. M. B., Willmersdorf, R. B., Lyra, P. R. M., Torres, J. V. S., de Andrade, E. Q., and Cunha, D. J. S. 2019. "Failure pressure prediction of corroded pipes under combined internal pressure and axial compressive force", *Journal of the Brazilian Society of Mechanical Sciences and Engineering*, vol. 41, no. 4.

Cabral, H. L. D., Motta, R. S., Afonso, S. M. B., Willmersdorf, R. B., Lyra, P. R. M., and de Andrade, E. Q. 2017. "The development of a computational tool for generation of high quality FE models of pipelines with corrosion defects", *Journal of the Brazilian Society of Mechanical Sciences and Engineering*, vol. 39, no. 8, p. 3137–50.

Cabral, H. L. D., Willmersdorf, R. B., Afonso, S. M. B., Lyra, P. R. M., and De Andrade, E. Q. 2007. "The development of a computational tool for generation of high quality FE models of pipelines with corrosion defects", *International Journal Of Modeling And Simulation For The Petroleum Industry*, vol. 1, no. 1, p. 9–21.

Chouchaoui, B., A. and Pick, R., J. 1996. "Behaviour of longitudinally aligned corrosion pits", *International Journal of Pressure Vessels and Piping*, vol. 67, nos. 0308–0161, p. 17–35.

Drumond, G. P., Pasqualino, I. P., Pinheiro, B. C., and Estefen, S. F. 2018. "Pipelines, risers and umbilicals failures: A literature review", *Ocean Engineering*, vol. 148, p. 412–25.

Fan, Z., Yu, J., Sun, Z., and Wang, H. 2017. "Effect of axial length parameters of ovality on the collapse pressure of offshore pipelines", *Thin-Walled Structures*, vol. 116, p. 19–25.

Ferreira, A. D. M., Motta, R. de S., Afonso, S. M. B., Willmersdorf, R. B., Lyra, P. R. M., de Andrade, E. Q., and Cunha, D. J. S. 2021. "Stochastic assessment of burst pressure for corroded pipelines", *Journal of the Brazilian Society of Mechanical Sciences and Engineering*, vol. 43, no. 4.

Fraldi, M., Freeman, R., Slater, S., Walker, A. C., and Guarracino, F. 2011. "An improved formulation for the assessment of the capacity load of circular rings and cylindrical shells under external pressure. Part 2. A comparative study with design codes prescriptions, experimental results and numerical simulations", *Thin-Walled Structures*, vol. 49, no. 9, p. 1062–70.

Fraldi, M. and Guarracino, F. 2011. "An improved formulation for the assessment of the capacity load of circular rings and cylindrical shells under external pressure. Part 1. Analytical derivation", *Thin-Walled Structures*, vol. 49, no. 9, p. 1054–61.

Gong, S., Wang, X., and Yuan, L. 2020a. "On the arresting performance of welded-ring buckle arrestor for subsea pipelines", *Ships and Offshore Structures*, vol. 15, no. 10, p.1057–69.

Gong, S., Zhou, L., Wang, X., Yuan, L., and Liu, C. 2020b. "On the influence of interacting dual defects on the collapse pressure of pipes under external pressure", *Thin-Walled Structures*, vol. 157.

Gong, S., Zhou, L., Wang, X., Yuan, L., and Liu, C. 2021. "On the collapse of thick-walled pipes with corrosion defects under external pressure", *Marine Structures*, vol. 76.

Idris, N. N., Mustaffa, Z., Ben Seghier, M. E. A., and Trung, N. T. 2021. "Burst capacity and development of interaction rules for pipelines considering radial interacting corrosion defects", *Engineering Failure Analysis*, vol. 121.

Kara, F., Navarro, J., and Allwood, R. L. 2010. "Effect of thickness variation on collapse pressure of seamless pipes", *Ocean Engineering*, vol. 37, p. 998–1006.

Li, X., Bai, Y., Su, C., and Li, M. 2016. "Effect of interaction between corrosion defects on failure pressure of thin wall steel pipeline", *International Journal of Pressure Vessels and Piping*, vol. 138, p. 8–18.

Liu, X., Zheng, J., Fu, J., Ji, J., and Chen, G. 2018. "Multi-level optimization of maintenance plan for natural gas pipeline systems subject to external corrosion", *Journal of Natural Gas Science and Engineering*, vol. 50, p. 64–73.

Mondal, B. C. and Dhar, A. S. 2017. "Interaction of multiple corrosion defects on burst pressure of pipelines", *Canadian Journal of Civil Engineering*, vol. 44, no. 8, p. 589–97.

Motta, R. S., Cabral, H. L. D., Afonso, S. M. B., Willmersdorf, R. B., Bouchonneau, N., Lyra, P. R. M., and de Andrade, E. Q. 2017. "Comparative studies for failure pressure prediction of corroded pipelines", *Engineering Failure Analysis*, vol. 81, p. 178–92.

Motta, R. de S., Leal, C. F., Ferreira, A. D., Afonso, S. M. B., Lyra, P. R. M., and Willmersdorf, R. B. 2021. "Reliability analysis of ovalized deep-water pipelines with corrosion defects", *Marine Structures*, vol. 77.

Netto, T. A. 2009. "On the effect of narrow and long corrosion defects on the collapse pressure of pipelines", *Applied Ocean Research*, vol. 31, no. 2, p. 75–81.

Netto, T. A., Ferraz, U. S., and Botto, A. 2007. "On the effect of corrosion defects on the collapse pressure of pipelines", *International Journal of Solids and Structures*, vol. 44, nos. 22–23, p. 7597–7614.

Papadakis, G. 2008. "Buckling of thick cylindrical shells under external pressure: A new analytical expression for the critical load and comparison with elasticity solutions", *International Journal of Solids and Structures*, vol. 45, no. 20, p. 5308–21.

Patran 2012. MSC Patran Library (PCL Manuals) and MSC. Acumen Library (Develop Manuals).

Pimentel, J. T., Marques Ferreira, A. D., de Siqueira Motta, R., Figueiroa da Silva Cabral, M. A., Maria Bastos Afonso, S., Brito Willmersdorf, R., Maciel Lyra, P. R., de Andrade, E. Q., and da Silveira Cunha, D. J. 2020. "New procedure of automatic modeling of pipelines with realistic shaped corrosion defects", *Engineering Structures*, vol. 221.

Qin, G. and Cheng, Y. F. 2021. "A review on defect assessment of pipelines: Principles, numerical solutions, and applications", *International Journal of Pressure Vessels and Piping*, vol. 191.

Riks, E. 1972. "The Application of Newton's Method to the Problem of Elastic Stability 1", *Journal of Applied Mechanics*, vol. 39, no. 4, p. 1060–65.

Sakakibara, N., Kyriakides, S., and Corona, E. 2008. "Collapse of partially corroded or worn pipe under external pressure", *International Journal of Mechanical Sciences*, vol. 50, no. 12, p. 1586–97.

Silva, R. C. C., Guerreiro, J. N. C., and Loula, A. F. D. 2007. "A study of pipe interacting corrosion defects using the FEM and neural networks", *Advances in Engineering Software*, vol. 38, nos. 11–12, p. 868–75.

Soares, E., Bruère, V. M., Afonso, S. M. B., Willmersdorf, R. B., Lyra, P. R. M., and Bouchonneau, N. 2019. "Structural integrity analysis of pipelines with interacting corrosion defects by multiphysics modeling", *Engineering Failure Analysis*, vol. 97, p. 91–102.

Wu, H., Zhao, H., Li, X., Feng, X., & Chen, Y. 2022. "Experimental and numerical studies on collapse of subsea pipelines with interacting corrosion defects", *Ocean Engineering*, vol. 260.

Xue, J. and Gan, N. 2014. "A comprehensive study on a propagating buckle in externally pressurized pipelines", *Journal of Mechanical Science and Technology*, vol. 28, no. 12, p. 4907–19.

Xue, J. and Hoo Fatt, M. 2002. "Buckling of a non-uniform, long cylindrical shell subjected to external hydrostatic pressure", *Engineering Structures*, vol. 24, p. 1027–34.

Yan, S. T., Shen, X. L., and Jin, Z. J. 2015. "On instability failure of corroded rings under external hydrostatic pressure", *Engineering Failure Analysis*, vol. 55, p. 39–54.

Ye, H., Yan, S., and Jin, Z. 2016. "Collapse of corroded pipelines under combined tension and external pressure", *PLoS ONE*, vol. 11, no. 4.

9. RESPONSIBILITY NOTICE

The authors are the only responsible for the printed material included in this paper.